

1 **Non-invasive ultrasound quantification of Scar Tissue Volume predicts functional changes during**
2 **tendon healing.**

3
4 Jessica E. Ackerman¹, Valentina Studentsova¹, Alayna E. Loiselle^{1,*}

5
6 ¹Center for Musculoskeletal Research, University of Rochester, Rochester, New York, United States of
7 America

8
9 *Corresponding Author

10 Alayna E. Loiselle, PhD

11 Center for Musculoskeletal Research

12 University of Rochester Medical Center

13 601 Elmwood Ave

14 Box 665

15 Rochester, NY

16 14642

17 Phone: 585-275-7239

18 Fax: 585-276-2177

19 Alayna_Loiselle@urmc.rochester.edu

20
21 **Running title: Ultrasound assessment of tendon healing**

22
23 **Key words:** tendon healing, ultrasound, scar tissue, mouse model, range of motion

24
25 **Author Contributions:**

26 Study conception and design: JEA, AEL; Acquisition of data: JEA, VS; Analysis and interpretation of data: JEA,

27 VS, AEL; Drafting of manuscript: JEA, AEL; Revision and approval of manuscript: JEA, VS, AEL.

28

29 **Acknowledgements:**

30 We would like to thank the Histology, Biochemistry and Molecular Imaging (HBMI) and the Biomechanics and
31 Multimodal Tissue Imaging (BMTI) Cores for technical assistance. Research reported in this publication was
32 supported by the National Institute of Arthritis and Musculoskeletal and Skin Diseases of the National Institutes
33 of Health under Award Numbers K01 AR068386, R01 AR073169, R21 AR073961 and P30 AR069655. The
34 content is solely the responsibility of the authors and does not necessarily represent the official views of the
35 National Institutes of Health.

36 **Abstract**

37 Tendon injuries are very common and disrupt the transmission of forces from muscle to bone, leading to
38 impaired function and quality of life. Successful restoration of tendon function after injury is a challenging
39 clinical problem due to the pathological, scar-mediated manner in which tendons heal. Currently, there are no
40 standard treatments to modulate scar tissue formation and improve tendon healing. A major limitation to the
41 identification of therapeutic candidates has been the reliance on terminal end-point metrics of healing in pre-
42 clinical studies, which require a large number of animals and result in destruction of the tissue. To address this
43 limitation, we have identified quantification of Scar Tissue Volume (STV) from ultrasound imaging as a
44 longitudinal, non-invasive metric of tendon healing. STV was strongly correlated with established endpoint
45 metrics of gliding function including Gliding Resistance (GR) and Metatarsophalangeal (MTP) Flexion Angle.
46 However, no associations were observed between STV and tensile mechanical properties. To define the
47 sensitivity of STV to identify differences between functionally discrete tendon healing phenotypes, we utilized
48 S100a4 haploinsufficient mice (S100a4^{GFP/+}), which heal with improved gliding function relative to wildtype
49 (WT) littermates. A significant decrease in STV was observed in S100a4^{GFP/+} repairs, relative to WT at day 14.
50 Taken together, these data suggest US quantification of STV as a means to facilitate the rapid screening of
51 biological and pharmacological interventions to improve tendon healing, and identify promising therapeutic
52 targets, in an efficient, cost-effective manner.

53

54

55

56 Introduction

57 Tendon injuries disrupt the transmission of forces from muscle to bone, leading to chronic pain,
58 disability and a large socioeconomic burden¹. Tendon injuries are very common, as there are over 300,000
59 tendon repair procedures a year in the United States², which result from either acute trauma or chronic
60 tendinopathy. While satisfactory outcome rates vary between tendons, successful restoration of tendon
61 function after injury remains a challenging clinical problem, with up to 40% of flexor tendon injuries healing with
62 functional limitations³. Unsatisfactory outcomes of surgical tendon repair procedures are due to the
63 pathological, scar-mediated manner in which tendons heal. Rather than regenerating native tendon tissue,
64 tendons heal via bridging scar tissue composed of a disorganized collagen extracellular matrix (ECM),
65 resulting in mechanical properties that are inferior to native tendon, and increasing the risk of re-injury or
66 rupture. Additionally, scar tissue impairs tendon range of motion (ROM), a particularly problematic complication
67 in the flexor tendons of the hands³.

68
69 Despite attempts using a variety of biological and tissue engineering approaches, there is currently no
70 consensus therapy to improve outcomes after tendon injury. An insufficient understanding of the underlying
71 mechanisms that contribute to scar-mediated tendon healing is a major impediment to the development of
72 successful therapies. To address this limitation, we developed a murine model of tendon injury and repair that
73 recapitulates many clinical aspects of healing including abundant scar tissue formation and impaired
74 restoration of mechanical properties⁴⁻⁶. However, progress in this field is limited by the absence of cost-
75 effective longitudinal outcome measures of tendon healing. Currently, we quantify impairments in gliding
76 function using end-point analyses of Gliding Resistance and measurement of the Metatarsophalangeal (MTP)
77 flexion angle after loading of the proximal FDL with small weights^{4,7}, consistent with large animal⁸ and
78 cadaveric studies⁹. This powerful technique has allowed us to define the temporal course of scar formation in
79 the murine model⁴, and demonstrated the effects of multiple genetic and pharmacological perturbations on the
80 healing process¹⁰⁻¹². However, these studies require many animals to properly power the study and to get
81 sufficient temporal resolution over the course of scar formation and healing. Thus, current approaches are
82 expensive, time-consuming and do not allow longitudinal evaluation or concomitant assessment of function
83 and tissue morphology in the same specimen. Therefore, our objective was to establish quantification of Scar

34 Tissue Volume from ultrasound (US) images as a longitudinal, non-invasive metric of tendon healing. US-
35 based quantification of tendon excursion will dramatically reduce the number of animals needed by
36 longitudinally assessing a single cohort of animals over the entire course of healing. Furthermore, US-based
37 characterization will provide more flexibility as we characterize novel genetic models and interventions as we
38 can image at many more time-points. In addition, while GR and MTP Flexion allow us to make assumptions
39 about tissue morphology, concomitant assessment of function and morphology are not possible in a single
40 specimen. In contrast, 3D reconstruction and segmentation of US images allow direct assessment and
41 quantification of tissue morphology. Finally, US is an ideal modality to longitudinally assess tendon healing, as
42 it is non-ionizing, and can be easily scaled between pre-clinical and clinical applications.

43 **Methods**

44 *Animal Ethics:* This study was carried out in strict accordance with the recommendations in the Guide for the
45 Care and Use of Laboratory Animals of the National Institutes of Health. All animal procedures were approved
46 by the University Committee on Animal Research (UCAR) at the University of Rochester (UCAR Number:
47 2014-004).

48 *Acute tendon injury and repair:* The following strains of mice were obtained from Jackson laboratories (Bar
49 Harbor, ME): C57BL6/J (#664) and S100a4^{GFP/+} and Wildtype (WT) littermates (#012904; B6.129S6-
50 S100a4^{tm1Egn/YunkJ}). Only female C57Bl/6J mice were used, while male and female S100a4^{GFP/+} and WT used
51 in equal proportions across genotypes. At 10-12 weeks of age, mice underwent surgical transection and repair
52 of the flexor digitorum longus (FDL) tendon in the hind paw as we have previously described^{4,10-14}. Briefly, the
53 distal FDL tendon was exposed and transected; two horizontal 8-0 sutures were placed in the intact tendon
54 ends and the tendon was sutured to approximate an end-to-end repair. The tendon was also transected
55 proximally along the tibia at the myotendinous junction to decrease strain on the repair.

56 *Ultrasound quantification of Scar Tissue Volume:* A high-frequency ultrasound platform (Vevo® 3100,
57 FUJIFILM VisualSonics Inc., Toronto, Canada), with a 70-MHz transducer probe (MX700; FUJIFILM
58 VisualSonics Inc., Toronto, Canada) was used for *in vivo* imaging of the healing tendon. For imaging studies,

12 mice were anesthetized with isoflurane, and placed in the prone position. The right hind paw was gently
13 secured proximal to tibiotalar (ankle) joint with surgical tape. After aligning the ultrasound probe with the
14 tendon at the mid-point of the hind paw, the hind paw was covered in ultrasound gel (Aquasonic 100, Parker,
15 Fairfield, NJ) and imaged. A total of 105 40 μ m-thick transverse B mode images were collected across the 4mm
16 region of interest (ROI), which included the entire width of the hind paw. All system settings, including gain
17 (96%), monitor dynamic range (70 dB), and depth (2 cm), were kept constant.

18 The same cohort of mice (n=9) underwent ultrasound imaging at 7, 14, 20, and 28 days post-surgery, followed
19 by assessment of gliding function and mechanical properties at day 28 (Figure 1A). Two mice were excluded
20 from analysis at day 28 due to failure during testing. An additional cohort of animals (n=7) underwent
21 ultrasound imaging at day 14, followed by sacrifice and assessment of gliding function and mechanical
22 properties.

23
24 *Segmentation and validation with histology:* B-mode images were exported as 3D volumes and loaded in to
25 AMIRA (FEI v.6.1.1, Thermo Scientific, Hillsboro, OR). The scar tissue boundaries were identified and
26 segmented on each slice. A 3D reconstruction of the scar tissue was generated and volumetrically quantified,
27 resulting in the Scar Tissue Volume (STV) metric. To validate the correct segmentation of STV in US images,
28 a subset of specimens (n=5) underwent both US imaging and histological evaluation. Following US imaging,
29 mice were sacrificed, and hind paws were harvested and fixed in 10% neutral buffered formalin (NBF) for 72
30 hours at room temperature. Samples were then decalcified for 7 days in 14% EDTA¹⁵ at room temperature
31 and processed for paraffin histology. Serial 5 μ m transverse sections were cut through the entire width of the
32 hindpaw that included the flexor tendon and/or scar tissue. For 3D reconstruction, sections corresponding to
33 every 40 μ m were stained with Alcian Blue/ Hematoxylin/ Orange G (ABHOG), as the step size of the US
34 images was 40 μ m. ABHOG was used as it allows easy discrimination between native tendon and scar tissue
35 ¹⁶. Stained sections were then digitally imaged, aligned, and stacked using NIH Image J ¹⁷, and loaded in to
36 AMIRA. Scar tissue was then manually segmented in each slice, and volumetrically quantified.

37
38 *Assessment of Gliding Function and Mechanical Testing:* Following ultrasound imaging, C57Bl/6J mice were
39 sacrificed at day 14 or day 28 post-surgery (n=7 per time-point) for assessment of gliding function and tensile

mechanical testing^{4,7,16}. The hindlimb was disarticulated at the knee and the skin was removed down to the ankle. The FDL tendon was isolated at the myotendinous junction and secured between two pieces of tape. The tibia was gripped in an alligator clip and the FDL was incrementally loaded with small weights from 0-19g. Digital images were taken after each weight was applied and the flexion angle at the metatarsophalangeal (MTP) joint was measured from these images. The MTP Flexion angle corresponds to the difference in flexion from the neutral, unloaded (0g) image, and the flexion angle when the 19g weight is applied. Application of a 19g weight results in complete flexion of uninjured FDL tendons. Gliding Resistance was calculated based on the changes in MTP Flexion Angle over the range of applied loads with higher Gliding Resistance indicating impaired gliding function. Following gliding assessment, tendons were released from the tarsal tunnel, the tibia and calcaneus were removed, and the repaired tendon underwent tensile testing as previously described^{4,7}. Briefly, the toes and the proximal end of the tendon were secured in opposing custom grips in an Instron 8841 uniaxial testing system (Instron Corporation, Norwood, MA) and tested in tension at a rate of 30mm/min, until failure.

Statistical Analyses: To identify significant differences in STV over time in C57BL/6J mice, a one-way Analysis of Variance (ANOVA) with post-hoc multiple comparisons was used. Student t-tests were used to identify significant differences between WT and S10a04^{GFP/+} repairs. Significance was set at $p < 0.05$. Two independent blinded observers performed all subjective readings (e.g. segmentation of STV, assessment of gliding function). Univariate regression analysis was used to determine if STV measured from ultrasound images correlated with gliding function or tensile mechanical properties. To evaluate intraoperator and interoperator error in the segmentation of STV, two operators measured 10 randomly selected C57BL/6J specimens. The average percent error was calculated as the absolute difference between measures divided by the average measurement. The coefficient of variance was calculated as previously described¹⁸. Percent error was also calculated between STV quantified from segmentation of histology and ultrasound in the same specimens.

Results

Segmentation and quantification of Scar Tissue Volume from ultrasound images

58 To determine whether tendon healing could be measured non-invasively using ultrasound, C57BL/6J mice
59 underwent complete transection and repair of the Flexor Digitorum Longus (FDL) tendon, and ultrasound
60 imaging was performed at 7, 14, 20, and 28 days post-surgery. High-frequency ultrasound permits the
61 identification of the healing (Figure 1C) FDL tendon in 2D sagittal B mode images. From these images,
62 discrete tissues can be segmented on each 2D slice (Figure 1D), including native tendon (pink), bone (green),
63 skin (yellow) and scar tissue (blue). Following segmentation, tissues were reconstructed in 3D (Figure 1E), and
64 Scar Tissue Volume (STV) was quantified (Figure 1E'). To determine the potential intra- and interoperative
65 sources of error in the quantification of STV. The average percent error between operators' measurements
66 was 15.6%, while the coefficient of variation was 16.6%.

67 68 *Histological validation of US segmentation of STV*

69 To confirm that US image segmentation for volumetric measurement was accurately identifying scar tissue we
70 analyzed 3D reconstructions of histological and US images from the same specimens and observed
71 comparable morphology when segmenting images from both modalities. In addition, volumetric quantification
72 of STV between modalities was highly consistent with a 10.8% error between US and histology segmentation.
73 Taken together, these data suggest our ability to properly identify and segment scar tissue via US imaging
74 (Fig. 2A-H).

75 76 77 78 79 80 81 82 83 84 85 86 *Scar Tissue Volume is strongly correlated with end-point metrics of gliding function*

87 No detectable scar tissue was observed in un-injured tendons. At day 7 post-surgery average STV was $0.96 \pm$
88 0.158mm^3 , with a subsequent increase on day 14 ($1.29 \text{ mm}^3 \pm 0.10$). Peak STV was observed at day 20 (1.55
89 $\text{mm}^3 \pm 0.19$) with a significant decrease observed at day 28 ($0.91 \text{ mm}^3 \pm 0.07$), relative to day 20 ($p < 0.05$)
90 (Figure 3A). To determine the relationship between STV and metrics of gliding function, univariate linear
91 regression analyses were performed. When day 14 and 28 data were grouped, a significant inverse
92 correlation was observed between STV and MTP Flexion Angle ($R^2=0.070$, $p=0.0002$) (Figure 3B), while a
93 significant, positive correlation was observed between STV and Gliding Resistance ($R^2=0.63$, $p=0.0007$)
94 (Figure 3C). However, when each timepoint was analyzed separately, stronger correlations were observed
95 between STV and gliding function at Day 14 and weaker, non-significant correlations were observed at day 28.

At Day 14, a strong, significant inverse correlation was observed between STV and MTP Flexion Angle ($R^2=0.82$, $p=0.005$), while a strong, significant positive correlation was observed between STV and Gliding Resistance ($R^2=0.71$, $p=0.01$). At Day 28 weak, non-significant correlations were observed between STV and MTP Flexion Angle ($R^2=0.46$, $p=0.09$) and Gliding Resistance ($R^2=0.36$, $p=0.15$) (Table 1). Taken together, these data suggest that STV is a significant indicator of gliding function during the earlier phases of tendon healing, but not during later healing.

Scar Tissue Volume does not predict tensile mechanical properties

To determine the potential relationship between STV and tensile mechanical properties, univariate linear regression analyses of STV and tensile mechanical properties (Stiffness, Max load at failure) were conducted. When days 14 and 28 were grouped there were no significant correlations between STV and Stiffness ($R^2=0.13$, $p=0.19$) (Figure 4A) or Max load ($R^2=0.05$, $p=0.68$) (Figure 4B). Furthermore, no significant associations were observed when each time-point was analyzed separately (Table 1), although a moderately strong but non-significant association was observed between STV and Stiffness at D14 ($R^2=0.54$, $p=0.06$).

STV identifies differences in models of fibrotic vs. regenerative healing

We have recently demonstrated that S100a4 haploinsufficiency (S100a4^{GFP/+}) results in improved gliding function and mechanical properties, relative to wildtype (WT) littermates¹⁹. To demonstrate the potential of STV to identify regenerative versus fibrotic models of tendon healing, STV was quantified at day 14 post-surgery. A significant 27% decrease in STV was observed in S100a4^{GFP/+} tendons, relative to WT ($p=0.0053$) (Figure 5), suggesting that STV has the sensitivity to non-invasively identify functional differences between modes of healing.

Discussion

Following injury, tendons are prone to a fibrotic, scar mediated healing process that both impairs restoration of range of motion and hinders the reacquisition of normal mechanical properties. Given that there are currently no biological approaches to improve the tendon healing process, there is a massive need for increased pre-clinical screening and identification of potential therapies. To address, we have identified Scar Tissue Volume

24 as a non-invasive ultrasound metric to determine the effects of genetic or pharmacological modifications on the
25 healing process, which may allow more rapid identification of tendon therapeutics. Importantly, this approach
26 has the potential to dramatically decrease the number of animals needed, consistent with the goals of reducing
27 the number of animals used in biomedical research²⁰. Moreover, non-invasive, longitudinal ultrasound imaging
28 can promote more rapid, cost-effective and high-throughput screening to facilitate the identification of
29 therapeutic targets.

30
31 Several studies have previously demonstrated the potential of using ultrasound to non-invasively image the
32 healing tendon. Ghorayeb *et al.*, quantified extracellular matrix content and found a strong correlation between
33 ECM content and linear stiffness in the Achilles tendon, although changes in range of motion were not
34 assessed. In the current study, we did not observe a significant association between STV and tissue stiffness,
35 although there was a moderately strong relationship at day 14 ($R^2=0.54$). While quantification of ECM and STV
36 may be similar in that both metrics are likely related to tissue size or bulk, which are related to impairments in
37 range of motion, differences in correlation with stiffness between ECM and STV may be due to differences in
38 the tissues that were quantified for ECM and STV, timing of analysis, or models of healing. In contrast to
39 quantification of tissue content or volume, several studies have examined the relationship between ultrasound
40 echogenicity and healing. Tamura *et al.*, used US echogenicity to assess healing in equine Superficial Digital
41 Flexor Tendons, although no change in echogenicity was observed despite longitudinal improvements in strain.
42 More recently, Lee *et al.*, assessed the relationship between US echogenicity, and tensile mechanical
43 properties in a collagenase-induced tendinopathy model and demonstrated that echo intensity was positively
44 correlated with maximum strain and stiffness²¹. Interestingly, tendon cross-sectional area and echogenicity
45 were increased in healing tendons, relative to controls. Although no correlation analysis was conducted
46 between these parameters, future studies will be needed to understand the potential relationship between STV
47 and echo intensity.

48
49 An important aspect of this approach is the ability to detect functional differences related to tendon ROM non
50 -invasively and over time. However, gait analysis can also be used to non-invasively assess restoration of

51 function during tendon healing²²⁻²⁴. While gait analysis is a strong metric in assessing Achilles and
52 supraspinatus
53 tendon healing in pre-clinical models, it is not yet known how alterations in gait correspond to flexor tendon
54 healing phases. Moreover, gait analysis parameters are typically associated with measurements of pain and
55 weakness, while the relationship between gait and tissue morphology are unknown. While we observe
56 changes
57 in STV over the course of healing, these differences are relatively modest, with no differences in STV observed
58 between 14- and 20-days post-surgery. However, we typically observe only slight differences in gliding function
59 metrics between these time-points⁴. Importantly, the real utility of end-point metrics of gliding
60 function is in identifying differences between genetically different strains of mice^{10,16},
61 or between pharmacological treatment groups¹¹ at a given timepoint. Taken together, these data
62 strongly suggest that longitudinal US based quantification of scar tissue volume may be utilized as a corollary
63 to
64 predict tendon ROM and gliding function during healing.

65
66 While STV strongly correlates with gliding function, there are several limitations to this study that must be
67 considered. STV does not correlate with mechanical properties, which are a critical indicator of the value of a
68 particular therapeutic intervention. Thus, future work seeks to develop multiple US-based metrics which either
69 alone or using multi-variate analyses may better correlate with restoration of mechanical properties.
70 Furthermore, we have only assessed healing in S100a4^{GFP/+} and WT mice at Day 14. However, we have
71 confined our analysis in these animals to day 14 due to the decrease in predictive power of STV at day 28.
72 Finally, while the goal of developing longitudinal, non-invasive metrics of healing is to permit rapid and cost-
73 effective therapeutic target screening, the segmentation process requires substantial expertise and is quite
74 time-consuming, thus to make this approach more high-throughput we will need to semi-automate or automate
75 the segmentation process.

76
77 Here we have shown that Scar Tissue Volume is significantly correlated with end-point metrics of gliding
78 function, and STV is particularly predictive of gliding function at Day 14, the period of peak impairments in

79 gliding function. In addition, STV is sensitive enough to discriminate between phenotypically distinct models of
30 healing. Future work will develop additional US-based metrics with the goal of non-invasive estimation of
31 mechanical properties. Taken together, this study identifies quantification of Scar Tissue Volume using
32 longitudinal, non-invasive ultrasound imaging as a novel means to assess tendon healing. This approach may
33 permit the rapid screening of biological and pharmacological interventions for healing, and identify promising
34 therapeutic targets, in an efficient, cost-effective manner.

References

- 1 Langer, R. & Vacanti, J. P. Tissue engineering. *Science* **260**, 920-926 (1993).
- 2 de Jong, J. P. *et al.* The incidence of acute traumatic tendon injuries in the hand and wrist: a 10-year population-based study. *Clinics in orthopedic surgery* **6**, 196-202, doi:10.4055/cios.2014.6.2.196 (2014).
- 3 Aydin, A. *et al.* [Single-stage flexor tendoplasty in the treatment of flexor tendon injuries]. *Acta Orthop Traumatol Turc* **38**, 54-59 (2004).
- 4 Loiselle, A. E. *et al.* Remodeling of murine intrasynovial tendon adhesions following injury: MMP and neotendon gene expression. *J Orthop Res* **27**, 833-840, doi:10.1002/jor.20769 (2009).
- 5 Ackerman, J. E. & Loiselle, A. E. Murine Flexor Tendon Injury and Repair Surgery. *J Vis Exp*, doi:10.3791/54433 (2016).
- 6 Ackerman, J. E. & Loiselle, A. E. in *International Combined Meeting of the Orthopaedic Research Society*.
- 7 Hasslund, S. *et al.* Adhesions in a murine flexor tendon graft model: Autograft versus allograft reconstruction. *J Orthop Res* **26**, 824-833 (2008).
- 8 Tanaka, T., Amadio, P. C., Zhao, C., Zobitz, M. E. & An, K. N. Gliding resistance versus work of flexion--two methods to assess flexor tendon repair. *J Orthop Res* **21**, 813-818, doi:10.1016/S0736-0266(03)00004-4 (2003).
- 9 Zhao, C., Ettema, A. M., Berglund, L. J., An, K. N. & Amadio, P. C. Gliding resistance of flexor tendon associated with carpal tunnel pressure: a biomechanical cadaver study. *J Orthop Res* **29**, 58-61, doi:10.1002/jor.21213 (2011).
- 10 Loiselle, A. E. *et al.* Bone marrow-derived matrix metalloproteinase-9 is associated with fibrous adhesion formation after murine flexor tendon injury. *PloS one* **7**, e40602, doi:10.1371/journal.pone.0040602 (2012).
- 11 Geary, M. B. *et al.* Systemic EP4 Inhibition Increases Adhesion Formation in a Murine Model of Flexor Tendon Repair. *PloS one* **10**, e0136351, doi:10.1371/journal.pone.0136351 (2015).
- 12 Orner, C. A., Geary, M. B., Hammert, W. C., O'Keefe, R. J. & Loiselle, A. E. Low-Dose and Short-Duration Matrix Metalloproteinase 9 Inhibition Does Not Affect Adhesion Formation during Murine Flexor Tendon Healing. *Plast Reconstr Surg* **137**, 545e-553e, doi:10.1097/01.prs.0000475823.01907.53 (2016).
- 13 Ackerman, J. E., Bah, I., Jonason, J. H., Buckley, M. R. & Loiselle, A. E. Aging does not alter tendon mechanical properties during homeostasis, but does impair flexor tendon healing. *J Orthop Res*, doi:10.1002/jor.23580 (2017).
- 14 Ackerman, J. E., Geary, M. B., Orner, C. A., Bawany, F. & Loiselle, A. E. Obesity/Type II diabetes alters macrophage polarization resulting in a fibrotic tendon healing response. *PloS one* **12**, e0181127, doi:10.1371/journal.pone.0181127 (2017).
- 15 Callis, G. & Sterchi, D. Decalcification of Bone: Literature Review and Practical Study of Various Decalcifying Agents. Methods, and Their Effects on Bone Histology. *Journal of Histotechnology* **21**, doi:<https://doi.org/10.1179/his.1998.21.1.49> (1998).
- 16 Ackerman, J. E., Best, K. T., O'Keefe, R. J. & Loiselle, A. E. Deletion of EP4 in S100a4-lineage cells reduces scar tissue formation during early but not later stages of tendon healing. *Sci Rep* **7**, 8658, doi:10.1038/s41598-017-09407-7 (2017).
- 17 Schneider, C. A., Rasband, W. S. & Eliceiri, K. W. NIH Image to ImageJ: 25 years of image analysis. *Nat Methods* **9**, 671-675 (2012).
- 18 Reynolds, D. G. *et al.* muCT-based measurement of cortical bone graft-to-host union. *Journal of bone and mineral research : the official journal of the American Society for Bone and Mineral Research* **24**, 899-907, doi:10.1359/jbmr.081232 (2009).
- 19 Ackerman, J. E., Studentsova, V., Best, K. T., Gira, E. & Loiselle, A. E. S100a4 promotes scar-mediated tendon healing via non-cell autonomous signaling. *In Review* (2018).
- 20 Flecknell, P. Replacement, reduction and refinement. *ALTEX* **19**, 73-78 (2002).
- 21 Lee, S. Y. *et al.* Characteristics of Sonography in a Rat Achilles Tendinopathy Model: Possible Non-invasive Predictors of Biomechanics. *Sci Rep* **7**, 5100, doi:10.1038/s41598-017-05466-y (2017).

- 36 22 Howell, K. *et al.* Novel Model of Tendon Regeneration Reveals Distinct Cell Mechanisms Underlying
37 Regenerative and Fibrotic Tendon Healing. *Sci Rep* **7**, 45238, doi:10.1038/srep45238 (2017).
38 23 Wang, Z. *et al.* A Mouse Model of Delayed Rotator Cuff Repair Results in Persistent Muscle Atrophy
39 and Fatty Infiltration. *Am J Sports Med*, 363546518793403, doi:10.1177/0363546518793403 (2018).
40 24 Bell, R., Taub, P., Cagle, P., Flatow, E. L. & Andarawis-Puri, N. Development of a mouse model of
41 supraspinatus tendon insertion site healing. *J Orthop Res* **33**, 25-32, doi:10.1002/jor.22727 (2015).
42

13 **Table 1.** Correlations between Scar Tissue Volume and Functional Metrics at 14 and 28 days post-surgery.

14
15 **Figure Legends**

16
17 **Figure 1. Quantification of Scar Tissue Volume from ultrasound images.** (A) Experimental design for
18 longitudinal ultrasound assessment of tendon healing at 7, 14, 20 and 28 days post-surgery, followed by
19 assessment of gliding function at day 28. An additional cohort of animals underwent ultrasound imaging only
20 at day 14, followed by either histological analysis, or assessment of gliding function. (B) Schematic of
21 ultrasound setup showing transverse plane of imaging. (C) 2D B Mode ultrasound image of a healing tendon at
22 day 14 post-surgery. (D) Segmentation of skin (yellow), metatarsal (green), FDL tendon (pink) and scar tissue
23 (blue) at day 14 post-surgery. (E) 3D Reconstruction of segmented tissues at day 14 post-surgery. (E') 3D
24 reconstruction and volumetric quantification of STV at day 14 post-surgery.

25
26 **Figure 2. Validation of Scar Tissue Segmentation using histology.** (A & B) 2-Dimensional transverse
27 Histological (A) and US (B) image sections from the same specimen. (C & D) Segmentation of scar tissue
28 (blue) and tendon (pink) from (C) histology, and (D) US images. (E & F) Following segmentation of all 2D
29 images containing scar tissue from (E) histology, and (F) US, the segmented slices were reconstructed in 3D,
30 and (G & H) scar tissue was volumetrically quantified.

31
32 **Figure 3. Scar Tissue Volume is correlated with changes in gliding function.** (A) Scar Tissue Volume was
33 quantified longitudinally at 7, 14, 20, and 28 days post-surgery. Peak STV was observed at day 20. (*)
34 indicates $p < 0.05$. (B-C) Linear regression analyses of STV and (B) MTP Flexion Angle, (C) Gliding Resistance
35 at 14 and 28 days. Circles represent Day 14 and squares represent day 28.

36
37 **Figure 4. Scar Tissue Volume is not correlated with tensile mechanical properties.** Linear regression
38 analyses of STV and (A) Stiffness, (B) Max load at failure at 14, and 28 days post-surgery. Circles represent
39 Day 14 and squares represent day 28.

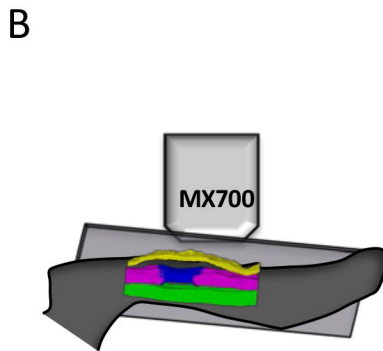
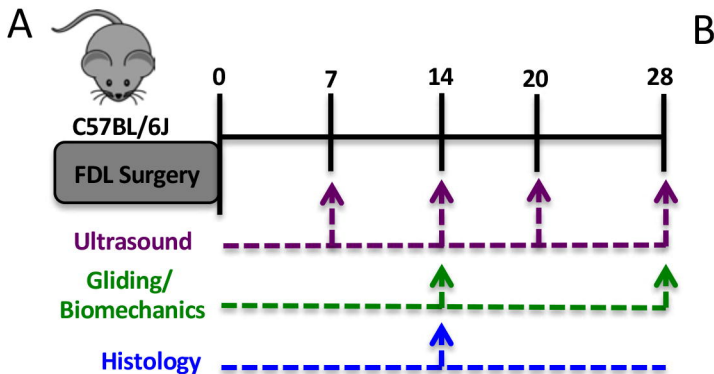
71 **Figure 5. Scar Tissue Volume identifies functional differences between models of scar-mediated and**
72 **regenerative tendon healing.** Quantification of Scar Tissue Volume in WT and S1004 haploinsufficient
73 (S100a4^{GFP/+}) tendon repairs at day 14 post-surgery. S100a4^{GFP/+} mice heal with improved gliding function and
74 decreased STV. (** indicates $p < 0.001$).

75

76

77

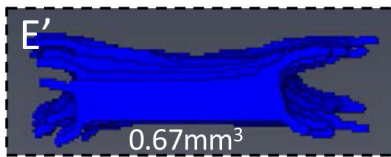
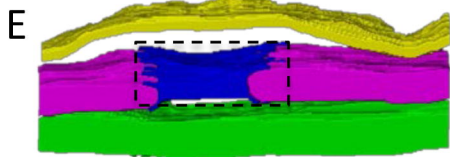
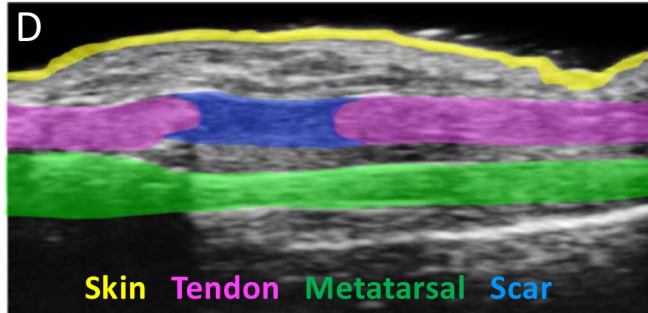
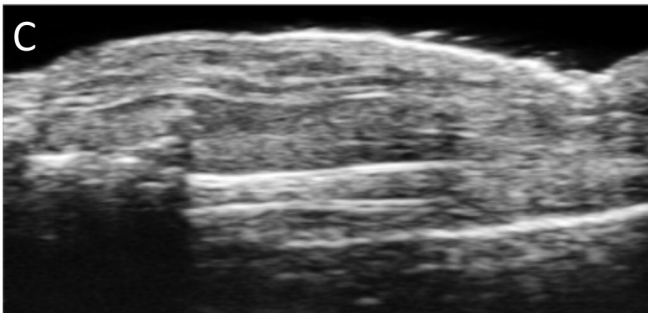
78



Day 14 Post-Surgery

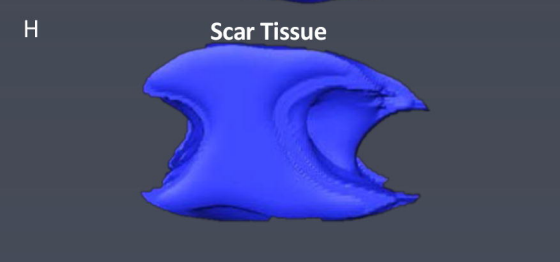
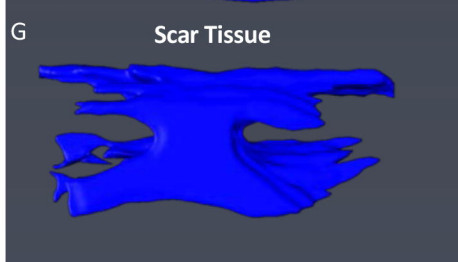
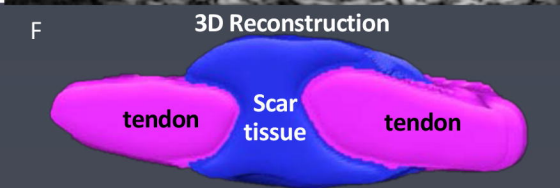
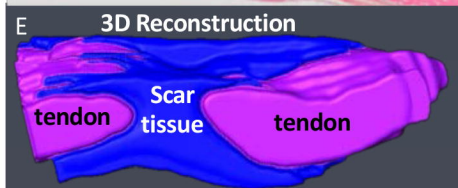
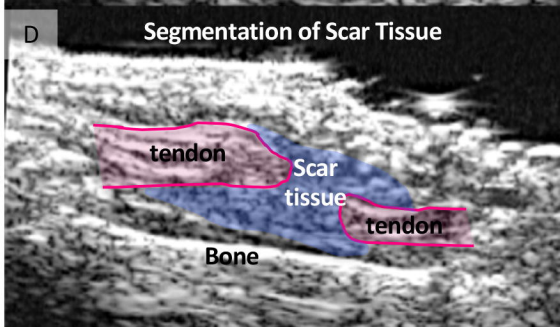
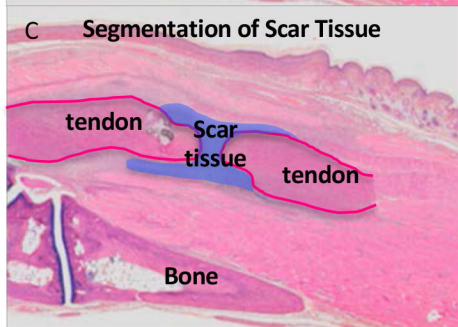
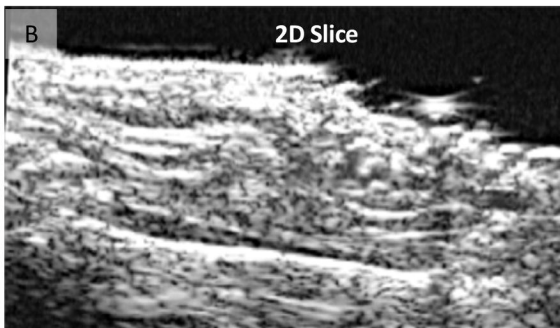
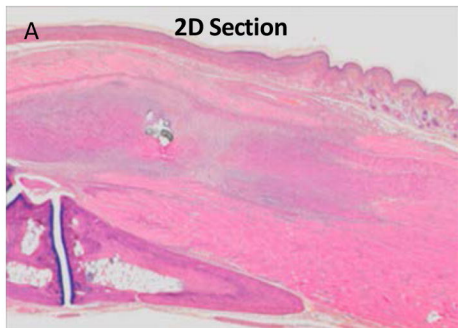
2D B mode ultrasound images

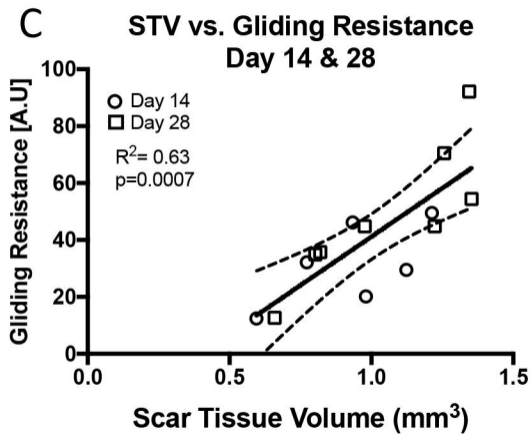
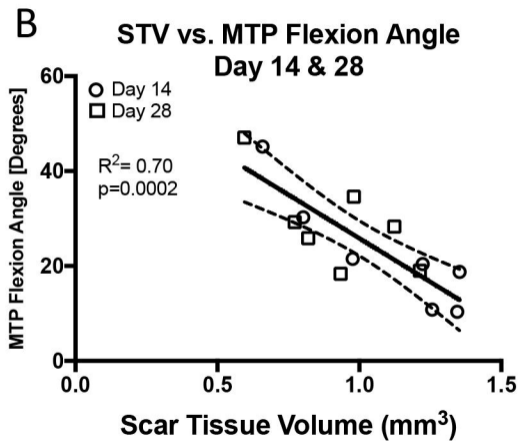
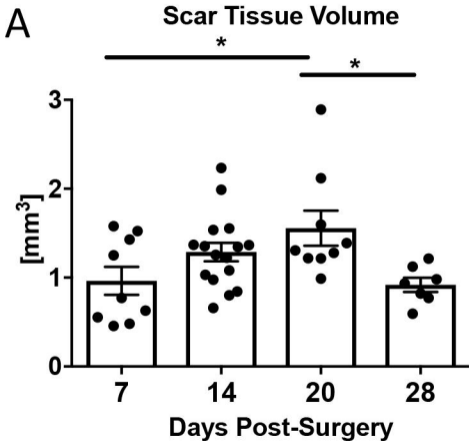
Tissue Segmentation

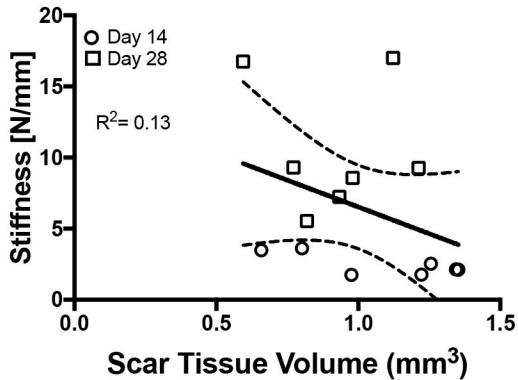
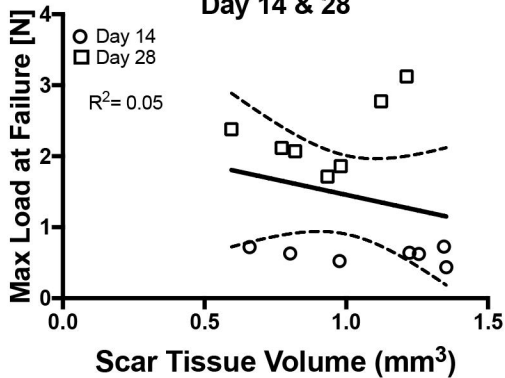


Histology

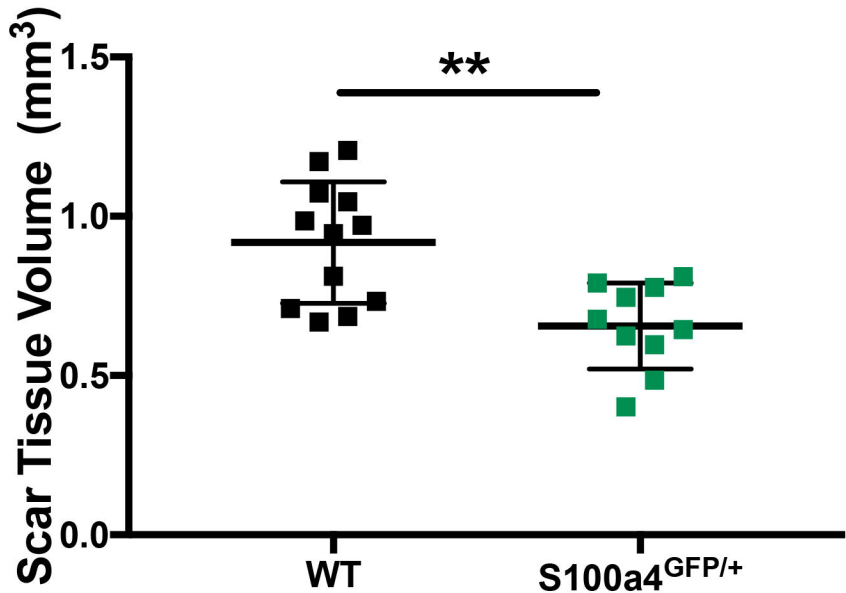
Ultrasound





A**STV vs. Stiffness
Day 14 & 28****B****STV vs. Max Load
Day 14 & 28**

Scar Tissue Volume



	Scar Tissue Volume			
	Day 14		Day 28	
	r	p value	r	p value
Gliding/ Biomechanics parameter				
Gliding Resistance	0.71**	0.01	0.36	0.15
MTP Flexion Angle	0.82**	0.005	0.46	0.09
Stiffness	0.54	0.06	0.009	0.83
Max load at failure	0.09	0.49	0.25	0.24